Ultrasonic study of normal-incommensurate-commensurate phase transitions in $[N(CH_3)_4]_2MnCl_4$

Pavol Kubinec,* Eriks Birks,† Wilfried Schranz, and Armin Fuith
Institute of Experimental Physics, University Vienna, Strudlhofgasse 4, A-1090 Vienna, Austria
(Received 1 June 1993)

The complete set of elastic constants of the single crystal $[N(CH_3)_4]_2MnCl_4$ has been measured at 15 MHz in the temperature range 250–310 K, including the normal-incommensurate transition at $T_I=292.3$ K, the incommensurate-improper ferroelastic lock-in transition at $T_L=291.7$ K, and the improper ferroelastic–improper ferroelastic transition at $T_1=266.7$ K. The Landau theory has been used to explain the experimental data. In addition, the attenuation of the longitudinal wave associated with the C_{11} mode was measured as a function of temperature and frequency (12.7–71 MHz) around T_I and analyzed in terms of a dynamic-scaling model. Above T_I the results agree with both three-dimensional-Ising and mean-field theory. In the commensurate phase the critical exponents have values consistent with mean-field theory. The relaxation time of the amplitudon below T_I has been determined to be $\tau_A=\tau_{A0}/(T_I-T)$ with $\tau_{A0}\approx 4\times 10^{-10}$ s K.

I. INTRODUCTION

Tetramethylammonium tetrachloromanganate $[N(CH_3)_4]_2MnCl_4$ (TMATC-Mn) belongs to the large A_2BX_4 family [where A=K, Rb, Cs, NH_4, and $N(CH_3)_4$; B=Se, Zn, Co, Mn, Ni, and Fe; and X=O, Cl, Br, and F] and undergoes, similarly to other members of this group, several phase transitions.[1–3] The sequence of phase transitions at atmospheric pressure is as follows:

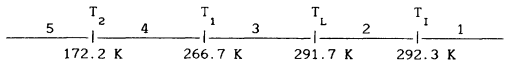

Phase 1, paraphase orthorhombic $D_{2h}^{16}(Z=4)-Pman$; phase 2, incommensurate $\mathbf{q}_0\sim(1-\delta)\mathbf{a}^*/2$; phase 3, commensurate monoclinic $C_{2h}^5(Z=8)-P112_1/a$, improper ferroelastic $\mathbf{q}_0=\mathbf{a}^*/2$; phase 4, commensurate monoclinic $C_{2h}^5(Z=12)-P2_1/n11$, improper ferroelastic $\mathbf{q}_0=\mathbf{a}^*/3$; phase 5, commensurate monoclinic $C_{2h}^5(Z=4)-P12_1/a1$, ferroelastic $\mathbf{q}_0=\mathbf{a}^*$. The crystallographic axes are labeled in agreement with international standards ($c<a<b$), where $a=12.333$ Å, $b=15.669$ Å, and $c=9.046$ Å (at $T=293$ K).

In the high-temperature "normal" (N) paraphase 1, the $MnCl_4$ tetrahedra are disordered and the structure is isomorphous[4] with that of $[N(CH_3)_4]_2ZnCl_4$. On passing through the narrow temperature range of the incommensurate (INC) phase 2, the tetrahedra become ordered. In the monoclinic commensurate (C) phase 3, the tetrahedra alternately take one of the two configurations of phase 1, leading to a doubling of the unit cell in the a direction. The threefold superstructure in phase 4 is characterized by the alternate rotation of the $MnCl_4$ tetrahedra about an axis parallel to the c axis.

The rather narrow incommensurate phase 2 was observed by x-ray diffraction measurements.[5] It is only ~ 0.6 K wide, and $\mathbf{q}_0$ is nearly constant at $0.483\mathbf{a}^*$.

Dielectric measurements[1,2] of TMATC-Mn revealed the similarity with other members of the tetramethylammonium tetrahalogenometal family, especially by the unified reduced p-T phase diagram. Optical investigations including measurements of birefringence and angle between the extinction position in different domains done by Fuith *et al.*[6] confirmed the existence of an INC phase, showed the temperature dependence of the order parameter, and proved the weak first-order character of the phase transition at T_L. Recently, Vlokh *et al.*[7] studied properties of the INC phase of TMATC-Mn under uniaxial mechanical stress. A model of successive transitions based on the free-energy calculations for TMATC-Mn was proposed by Mashiyama[8] and Mashiyama and Tanisaki.[5]

Because of the ferroelastic nature of three successive phases, appreciable effects on the elastic properties are expected. Vlokh, Kityk, and Mokryi[9] reported on the influence of hydrostatic pressure on the birefringence and elastic data (C_{11}, C_{44}, C_{55}, and C_{66}). An abrupt change of the temperature dependence of C_{44} by high pressure was explained by a shift of the point of condensation of the soft mode in the Brillouin zone from $(1-\delta)\mathbf{a}^*/2$ to $(1-\delta)\mathbf{a}^*/3$. Relaxation time values of the non-Goldstone phason $\tau_\phi=(3.7-15)\times 10^{-11}$ s have been obtained for pressures between 170 and 250 MPa.

Concerning the dynamics at normal pressure, the relaxation time of the amplitudons and fluctuation effects were studied recently in another material of the tetramethylammonium tetrahalogenometal family, in $[N(CH_3)_4]_2ZnCl_4$ by impulsive stimulated scattering.[10] These measurements, which extended earlier ultrasonic measurements,[11] were analyzed in terms of a dynamical scaling theory of Fossum.[12]

In order to complete the elastic studies in TMATC-Mn, we have performed ultrasonic measurements of all main-diagonal components of the elastic stiffness tensor C_{ii} ($i=1,2,\ldots,6$) in the temperature range including the three phase transitions at T_I, T_L, and T_1. In addition, we have studied the frequency dependence of the at-

tenuation of the longitudinal wave associated with the C_{11} mode near T_I, from which the relaxation time of the amplitudon, τ_A, was determined. Part of our results connected with the acoustic dispersion were presented elsewhere.[13]

II. EXPERIMENTAL PROCEDURE

Single crystals of TMATC-Mn were grown by slow evaporation at (35±0.003) °C from an aqueous solution of the threefold recrystallized compounds $N(CH_3)_4Cl$ and $MnCl_2 \cdot 4H_2O$.[6] The samples for the ultrasonic experiments were of good optical quality and were cut with a diamond saw. The orientation of the crystal was obtained using a polarizing microscope. The samples were prepared by grinding with Al_2O_3 powder of sizes 12.5, 5, and 3 μm in Diaplastol as a lapping fluid. The accuracy of the linear dimension along the crystallographic axes was better than ±2 μm, and the end planes were parallel to within 1×10^{-3} rad. The accuracy of the orientation was better than ±1°. The sample dimensions were about 4 mm×4 mm×4 mm; the density of the samples was determined to be 1.327 g cm^{-3} by the Archimedes method.

Overtone-polished 15-MHz Y- and X-cut $LiNbO_3$ transducers (diameter 0.125 in.) from Valpey Fisher were bonded to the (100), (010), and (001) faces of the sample by using glycerin and epoxy, respectively, for measurements of the complete set of the elastic constants C_{ii} ($i=1,\ldots,6$). The specimen was mounted in the sample chamber with controlled temperature gradient along the sample.[14] The measurements were performed by increasing or decreasing the temperature at a rate of about 0.05 K min^{-1} using either the manual pulse echo overlap method with one transducer[15] or a home-built automated apparatus.[16] The values for attenuation were measured manually.

Overtone polished 10-MHz Y-cut $LiNbO_3$ transducers were used at their fundamental, third, fifth, and seventh harmonics for further measurements of the dynamical properties of a longitudinal wave propagating in the [100] direction around T_I. The ultrasonic attenuation coefficient was measured together with the velocity by using the exponential comparator method.[17] The reflected pulses have shown a good exponential decay pattern in the whole temperature range. In the vicinity of phase transitions, where the ultrasonic attenuation becomes large and only one echo could be observed (for higher frequencies), the relative attenuation was determined by measuring the change of the height of this first echo with temperature.

The temperature of the sample was determined using a platinum resistance thermometer of resistance 100 Ω at 273 K with an absolute accuracy of ±0.5 K and relative accuracy of ±0.005 K.

III. RESULTS

The results of our ultrasonic measurements are presented in Fig. 1 showing the longitudinal components of the elastic stiffness tensor C_{11}, C_{22}, and C_{33} as a function of temperature, and in Fig. 2 where the shear components C_{44}, C_{55}, and C_{66} are shown. The appearance of the incommensurate phase manifests itself in a dip at T_I in all longitudinal components C_{ii}, while the temperature dependence of transversal waves shows considerable changes only in C_{66} and C_{44}. The commensurate-commensurate phase transition at $T_1=266.7$ K leads to a pronounced jump in all components of elastic constants. The first-order character of this phase transition manifests itself in the temperature hysteresis of about 0.5 K (Figs. 1 and 2). The attenuation showed an anomalous behavior near the normal-incommensurate phase transition for C_{11}, C_{22}, C_{33}, and C_{66} only.

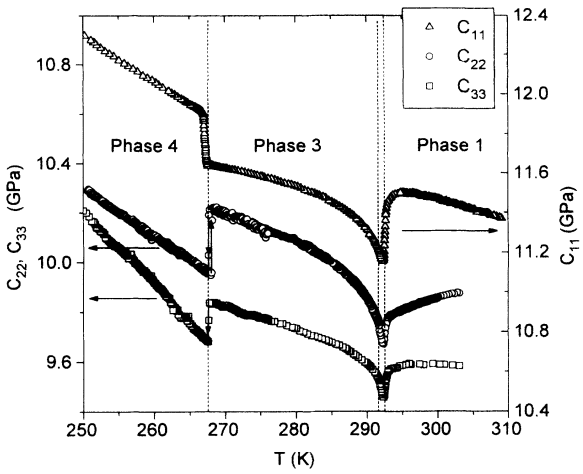

FIG. 1. Elastic constants of TMATC-Mn for longitudinal waves measured at 15 MHz.

As one can see from the detailed temperature dependence of the elastic constant C_{11} measured at 12.7 MHz (Fig. 3), there is a steplike change of C_{11} only at the transition temperature T_I and no change at the lock-in temperature T_L. This is consistent with the Landau theory of these phase transitions (see below).

The temperature and frequency dependence (12.7–71 MHz) of the attenuation α of the C_{11} mode near the N-

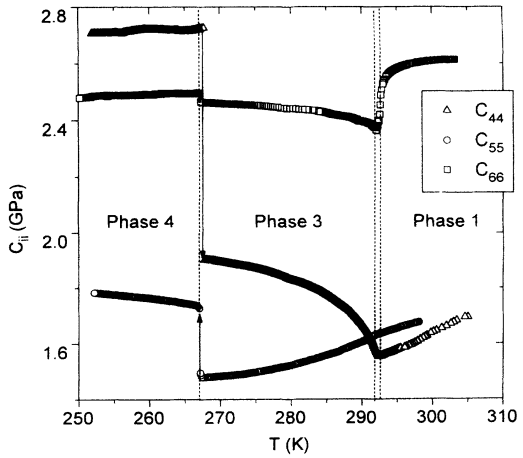

FIG. 2. Elastic constants of TMATC-Mn for transversal waves measured at 15 MHz.

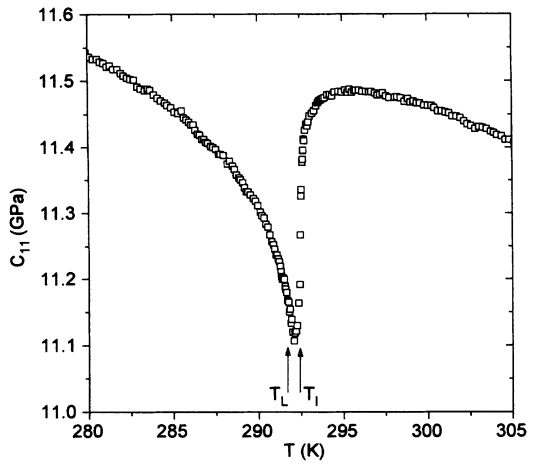

FIG. 3. Temperature dependence of the elastic constant C_{11} at 12.7 MHz around the normal-incommensurate phase transition.

INC-C phase transition is shown in Fig. 4. Here one can see a shift of narrow attenuation peaks toward lower temperatures with increasing frequency.

In order to extract only the anomalous part of the attenuation associated with the phase transition, the so-called critical attenuation α_{crit}, we have subtracted the constant background α_0 from the measured values α. The values of α_0 were taken from the attenuation coefficients at much higher temperatures and were 1.8, 3.5, 4.5, and 6.5 dB/cm for 12.7, 31, 51, and 71 MHz, respectively. The dependence of α_{crit}/f^2 is shown in Fig. 5. As one can see from Fig. 5, the values for α_{crit}/f^2 are independent of the applied frequency for $|T-T_I|>0.5$ K and show a dispersion in the very vicinity of T_I. This indicates that the relation $\omega\tau \ll 1$ fails close T_I. The measured data will now be further discussed on the basis of the Landau-Levanyuk theory.

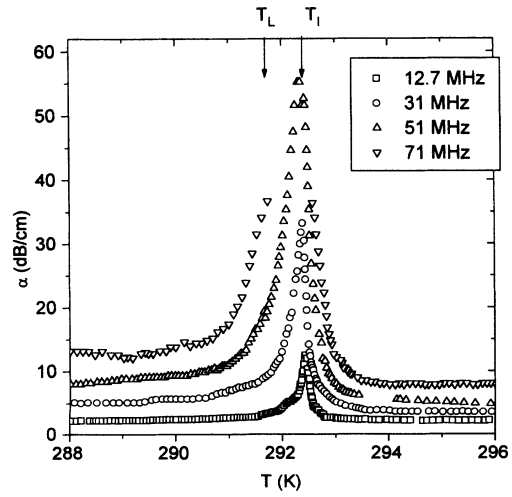

FIG. 4. Temperature dependence of the sound attenuation α for a longitudinal wave propagating along the [100] direction for various frequencies.

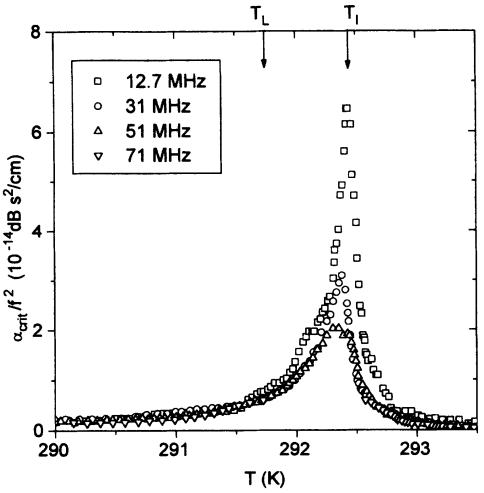

FIG. 5. Temperature dependence of the critical sound attenuation α_{crit}/f^2 for a longitudinal wave propagating along the [100] direction around the normal-incommensurate phase transition T_I for various frequencies.

IV. REVIEW OF THE THEORY

A. Landau theory for TMATC-Mn

The Landau free-energy density for the phase transitions in TMATC-Mn including the corresponding interaction terms between strain u_i and order parameter components Q and Q^* can be written[9]

$$\begin{aligned} F=&\tfrac{1}{2}AQ_qQ_q^*+\tfrac{1}{4}BQ_q^2Q_q^{*2}+\tfrac{1}{6}DQ_q^3Q_q^{*3}+\tfrac{1}{2}A'R_{q'}R_{q'}^* \\ &+\beta_1(Q_q^3R_{q'}^*+Q_q^{*3}R_{q'})+\beta_3(Q_{1/3}^3+Q_{1/3}^{*3})u_4 \\ &+i\beta_4(Q_0-Q_0^*)u_5+i\beta_2(Q_{1/2}^2-Q_{1/2}^{*2})u_6 \\ &+a_iQ_qQ_q^*u_i+\tfrac{1}{2}b_{ij}Q_qQ_q^*u_iu_j+\tfrac{1}{2}C_{ij}u_iu_j\ , \end{aligned} \tag{1}$$

where $R_{q'}=(-\beta_qQ_q^3/A')$ is the normal coordinate of the hard mode with a wave vector $q'=3q-1$, $A=A_1(T-T_I)+K(q-q_0)^2$, and $Q_{1/2}$, $Q_{1/3}$, and Q_0 are the normal coordinates of the soft-mode phasons in phases 3, 4, and 5, respectively.

Substituting the normal coordinates of the incommensurate phase, which are the amplitudons and phasons, one can derive the relations for the change of the elastic constant and attenuation near the T_I point,[18,9]

$$\Delta C_{ii}=-\frac{2a_i^2Q_0^2}{\omega_A^2(1+\omega^2\tau_A^2)}+b_{ii}Q_0^2\ , \tag{2}$$

$$\Delta\alpha_{ii}=(1/\rho v_{ii}^2)\frac{a_i^2Q_0^2}{\omega_A^2(1+\omega^2\tau_A^2)}(\omega^2\tau_A)\ . \tag{3}$$

In the INC phase, the frequency of the amplitudon is given by $\omega_A^2(q_0)=2A_1(T_I-T)$. The relaxation time of the order parameter $\tau_A=\Gamma_A/\omega_A^2$ and the order parameter is given by $Q_0^2=A_1(T_I-T)/B$. ω is the ultrasonic frequency, ρ is the density of the crystal, $a_i\neq 0$ for $i=1,2,3$, and $b_{ii}\neq 0$ for $i=1,\ldots,6$.

The Eqs. (2) and (3) are valid also in the C phase.

However, when analyzing the data in the C phase, one should use[19] $\omega_A^2(q_{1/2})=2A_1(T_0-T)$ and $Q_0^2=A_1(T_0-T)/B$, where $T_L<T_0<T_I$.

The first term in Eq. (2) yields a negative jump at T_I since the temperature dependences of Q_0^2 and ω_A^2 are the same. The second term leads to a change of slope at T_I with ΔC proportional to $Q_0^2\sim(T_I-T)$. The relaxation time of the amplitudon, τ_A, has a temperature dependence given by

$$\tau_A=\tau_{A0}/(T_I-T) \tag{4a}$$

and

$$\tau_A=\tau_{A0}/(T_0-T) \tag{4b}$$

in the INC and C phases, respectively.

From Eq. (3) one can see that the attenuation should be anomalous for longitudinal waves only. This is consistent with the experimental data; the anomaly in C_{66} arises due to the additional coupling term $i\beta_2(Q_{1/2}^2-Q_{1/2}^{*2})u_{xy}$ in Eq. (1). Following the procedure of Lemanov and Esayan,[18] one obtains

$$\Delta C_{66}=-\frac{2\beta_2^2Q_0^2}{\omega_R^2(1+\omega^2\tau_R^2)}+b_{66}Q_0^2\ , \tag{5}$$

$$\Delta\alpha_{66}=(1/\rho v_{66}^2)\frac{\beta_i^2Q_0^2}{\omega_R^2(1+\omega^2\tau_R^2)}(\omega^2\tau_R)\ , \tag{6}$$

where ω_R^2 and τ_R are the frequency and relaxation time of the upper hard mode.[20]

B. Dynamic scaling theory

The phenomenological analysis of ultrasound near phase transitions by Fossum[12] will be adopted here to describe the fluctuation contribution both below and above T_I.

For investigation of the fluctuation effect, one usually starts with the data from the paraphase. The critical fluctuation contribution to the velocity and attenuation is then given as[12,21]

$$\bar{v}\,\Delta v=A^+t^{-\mu}(1+Dt^{0.5})G(\omega\tau^+,\mu)\ , \tag{7}$$

$$v^3\,\Delta\alpha/\omega=(\mu/z\nu)A^+t^{-\mu}(1+Dt^{0.5})\omega\tau^+F(\omega\tau^+,\mu)\ , \tag{8}$$

where $\bar{v}=(v+v^0)/2\sim$const, $t=|T-T_I|/T_I$ is the reduced temperature, $1+Dt^{0.5}$ gives the leading correction to scaling, $\tau^+=\tau_0^+t^{-z\nu}$ is the critical relaxation time, and $G(\omega\tau,\mu)$ and $F(\omega\tau,\mu)$ are scaling functions given by the analytical approximation to the real and imaginary parts of the relaxation function $(1-i\omega\tau)^{-\mu/\nu z}$. The critical exponent $\mu=\alpha+2(\phi-1)$, where $\phi=1$ for non-symmetry-breaking sound modes.

In the "ordered" phase ($T<T_I$), the velocity and attenuation contributions are

$$\bar{v}\,\Delta v=A^-t^{-\mu}(1+Dt^{0.5})G(\omega\tau^-,\mu)+B^-t^{2\beta-\gamma}G(\omega\tau^{\mathrm{LK}},\gamma)\ , \tag{9}$$

$$v^3\,\Delta\alpha/\omega=(\mu/z\nu)A^-t^{-\mu}(1+Dt^{0.5})\omega\tau^-F(\omega\tau^-,\mu)+(\gamma/z\nu)B^-t^{2\beta-\gamma}\omega\tau^{\mathrm{LK}}F(\omega\tau^{\mathrm{LK}},\gamma)\ , \tag{10}$$

where $t=|T_I-T|/T_I$ and $t=|T_0-T|/T_0$ in the INC and C phases, respectively. The first terms describe the fluctuation contribution and the second term the Landau-Khalatnikov (LK) contribution. The relaxation time τ^{LK} corresponds to the relaxation time of the amplitudon, τ_A; in the mean-field approximation, $\tau_A=T_I\tau^{\mathrm{LK}}$. The exponents β and γ are the static critical exponents for the order parameter and susceptibility. Since this theory is phenomenological, the critical exponents can be viewed as effective values describing the range of data fitted and may differ from the expected asymptotic values.

The amplitude of fluctuations A^- below T_I is related to the amplitude A^+ in the paraphase. The A^-/A^+ ratio equals 1.85 for the three-dimensional- (3D-) Ising universality class, 0.97 for the 3D-XY universality class,[22] and 1.00 for the Landau mean-field theory.[23] The relaxation time τ^- has the same critical exponent $z\nu$ as τ^+ and the amplitude $\tau_0^-=\frac{1}{2}\tau_0^+$ in the conventional Van Hove dynamics ($z\nu=1$).

The theoretical analysis of Cowley and Bruce[24] predicts that critical behavior at the normal-incommensurate phase transition should correspond to the 3D-XY universality class. This would imply that $\mu=\alpha=-0.026$, $z\nu=1.36$, $\beta=0.345$, and $\gamma=1.316$. Previous analysis[22] of the acoustic anomalies at ultrasonic frequencies in Rb_2ZnCl_4, which belongs to the A_2BX_4 family, has shown that the critical exponents are more consistent with the 3D-Ising model ($\mu=\alpha=0.11$, $z\nu=1.28$, $\beta=0.324$, and $\gamma=1.24$). However, some problems arose there connected with the dynamical critical exponent $z\nu$, which was consistent with the Van Hove value $z\nu=1$ rather than the 3D-Ising value $z\nu=1.28$. Finally, the analysis in TMATC-Zn (Ref. 10) is consistent with the mean-field theory ($\mu=\alpha=0.5$, $z\nu=1$, $\beta=0.5$, and $\gamma=1$), although the data above T_I can be fitted to the 3D-Ising model, too.

V. DATA ANALYSIS

Our experimental data can be qualitatively described by the Landau theory as outlined above. Nevertheless, Eqs. (2) and (3) are mean-field results and describe the change of the elastic constant only due to the relaxation processes of the order parameter (and its coupling to the strain). For a more detailed description of the phase transition, one has to account for the fluctuation contribution. This affects the results both below and above T_I, contrary to the relaxation part which is effective only below T_I. The fluctuation contribution is usually smaller than the relaxation one (also here, see Fig. 4) and its influence on ΔC and $\Delta\alpha$ below T_I is often neglected.[18] Strictly speaking, we should subtract this part to obtain the mean-field results, but at the first step we will not do this, being satisfied with the first approximation only. We will return to the problem of fluctuations later.

A. Mean-field analysis

Concerning the longitudinal waves near T_I, one can easily calculate the ratio a_i^2/B (Fig. 1). The result

$a_1^2:a_2^2:a_3^2=3.5:1.6:1.4$ shows that the coupling is the largest for the a direction. Therefore we have used this direction for the investigation of the dynamics near T_I. The coefficients b_{ii} are positive for both $\mathbf{q}_0=\mathbf{a}^*/2$ and $\mathbf{q}_0=\mathbf{a}^*/3$, as follows from the temperature dependence of C_{ii} below T_I and T_1. The first-order character of the commensurate-commensurate ferroelastic phase transition at T_1 is demonstrated by the discontinuous change of C_{ii} at T_1 and the depression of the fluctuation region.

The transverse elastic constants C_{44} and C_{55} are described by Eq. (2), while C_{66} is determined by Eq. (5). From the temperature dependence of C_{44}, the critical exponent of the order parameter β can be calculated. With $Q_0^2\sim(T_I-T)^{2\beta}$ we have determined $2\beta=0.62\pm0.05$ in a wide temperature range. Strictly speaking, when analyzing the data in the C phase one should use $Q_0^2\sim(T_0-T)^{2\beta}$, where $T_L<T_0<T_I$. However, because of the smallness of the INC region, this does not cause a significant difference. The value of 2β is consistent with the value determined by birefringence[9] and similar to other crystals of the A_2BX_4 family.[18] This value differs from the mean-field theory value ($2\beta=1$) and may indicate the necessity of using higher terms in the Landau free-energy expansion (see, e.g., Ref. 25). The values $b_{44}>0$, $b_{55}\leq 0$, and $b_{66}\geq 0$ are effective in both phases 3 and 4. The slight decrease of C_{55} above T_I can be attributed to the bilinear coupling term $i\beta_4(Q_0-Q_0^*)u_5$, indicating that the value of C_{55}^0 is somewhat higher. Because of the steep changes in the elastic constants near T_1, the absolute values of C_{44} and C_{66} in phase 4 were not determined unambiguously.

Before we analyze the dynamics of the acoustic anomalies quantitatively, we have to determine the transition temperature T_I. Within the framework of the Landau-Khalatnikov theory, the temperature T_m at which the maximum in the acoustic attenuation occurs is a linear function of the acoustic frequency, given by the equation

$$T_m=-\tau_{A0}\omega+T_I\ . \tag{11}$$

A plot of T_m versus ultrasonic frequency ω is shown in Fig. 6. A fit to these points using Eq. (11) is also shown. The transition temperature determined from this fit is $T_I=(292.45\pm0.01)$ K. T_I will be fixed at this value for the further analysis of the data. It should be noted that the contribution of the energy-density fluctuations, which is addressed below, has very little effect on the position of the attenuation maximum below T_I and therefore the value of T_I determined from considering the LK contribution only is correct also in the presence of fluctuations. (There is a shift in T_I of about 0.02 K toward lower temperatures when accounting for fluctuations.)

Using Eq. (11), one can calculate the relaxation time of the amplitudons, τ_A. From the shift of the attenuation maximum (Fig. 6), one obtains $\tau_{A0}=(3.9\pm0.6)\times10^{-10}$ s K.

The relaxation time τ_A is large enough to manifest itself in the dispersion of the attenuation. Figure 5 shows the temperature dependence of the critical part of the attenuation divided by the square of the frequency, $\alpha_{\rm crit}/f^2$. It is important to note that the condition $\omega\tau_A\ll1$ fails to hold for $T_I-T<0.5$ K and the dispersion manifests itself not only in the shift of the attenuation maximum, but also in the different height of this critical part of attenuation. These results are consistent with the theoretical curve obtained from Eq. (3), which is shown in Fig. 7. Here we have taken $\tau_A=\tau_{A0}/(T_I-T)$ with $\tau_{A0}=3.9\times10^{-10}$ s K.

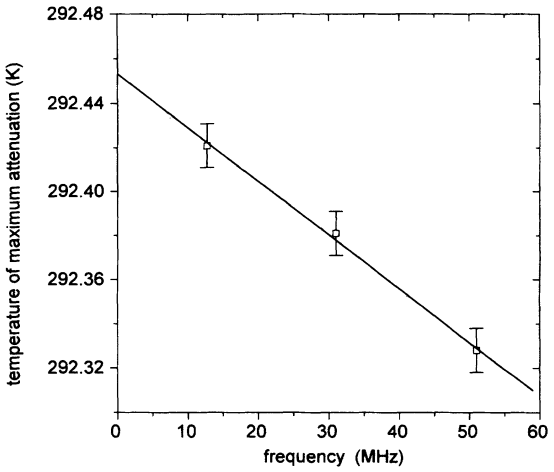

FIG. 6. Frequency dependence of the temperature T_m of the attenuation maximum.

Analogously, the dispersion should also appear in the ultrasonic velocity, but we were not able to measure the velocity very close to T_I for higher frequencies because of the high attenuation of the signal.

To compare our results to those in similar materials,[10,22,26] we note that the relaxation time is approximately the same as in Rb_2ZnCl_4 ($\tau_{A0}=6.8\times10^{-10}$ s K) or $[N(CH_3)_4]_2ZnCl_4$ ($\tau_{A0}=1.8\times10^{-10}$ s K). However, in $[N(CH_3)_4]_2ZnCl_4$ the authors[11] did not observe a dispersion in ultrasonic experiments because they were not able to measure the attenuation close enough to T_I for higher

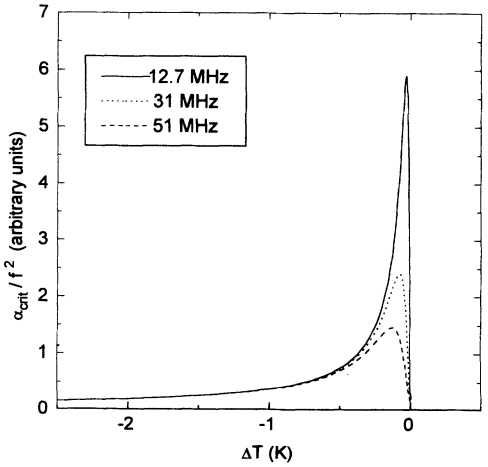

FIG. 7. Theoretical behavior of the relaxational part of the critical attenuation $\alpha_{\rm crit}/f^2$ near the INC phase transition T_I calculated from Eq. (3) for $\tau_{A0}=3.9\times10^{-10}$ s K^{-1} and various frequencies.

frequencies.

Now we comment on the fluctuation effect in our data.

B. Fluctuation effects

The above analysis has shown that the Landau mean-field theory describes the experimental data quite well. Nevertheless, there can arise a question whether other models (3D-Ising or 3D-XY) are more suitable or not. The fit of our velocity and attenuation data for $T > T_I$ according to Eqs. (7) and (8) in the limit $\omega\tau \ll 1$ leads to parameters which are sensitive on the background velocity and attenuation values as well as on the width of the fitted temperature range. Satisfactory fits can be obtained with parameters $\mu = 0.1-0.5$, $z\nu = 0.9-1.5$, and $\tau^+ = (4-7)\times 10^{-10}$ s K/$(T-T_I)$. The results are consistent with the 3D-Ising model and mean-field theory but not with the 3D-XY model, which requires $\mu = -0.007$. Figure 8 shows the fit of our data with the mean-field exponents $\mu = 0.5$, $z\nu = 1$, and $\tau^+ = 6\times 10^{-10}$ s K/$(T-T_I)$.

The results obtained from the attenuation $\alpha_{\rm crit}/\omega^2$ below T_I indicate that the mean-field model is the most appropriate at least for temperatures below T_L (Fig. 9). Because of the smallness of the INC region, it is difficult to draw definite conclusions about the critical exponents in the INC phase. Because of $\alpha_{\rm fl} \ll \alpha^{\rm LK}$ (for $T_I - T > 0.2$ K), one can write $\alpha_{\rm crit} = \alpha^{\rm LK} + \alpha_{\rm fl} \cong \alpha^{\rm LK}$. According to this model, $\alpha_{\rm crit}/\omega^2 \propto t^{-1}$ in the limit $\omega\tau \ll 1$, which agrees with the experimental results (Fig. 9). The exponents of $\alpha_{\rm crit}/\omega^2$ for the 3D-Ising and 3D-XY models are $2\beta-\gamma-z\nu = 1.87$ and 1.98, respectively, and do not describe the data below T_L. In the INC phase, a further analysis of the data is hampered by the crossover from $\omega\tau \ll 1$ to $\omega\tau > 1$ (Fig. 9).

Taking into account the fluctuation contribution for $T > T_I$, one can reinvestigate the results for $T < T_I$ more attentively. We have tried two cases: At first, we have assumed that the ratio between the magnitudes of the fluctuation contribution below T_I and above T_I is given by $A^-/A^+ = 1.85$, according to the 3D-Ising model. Then, subtracting the fluctuation contribution from the attenuation data for $T < T_I$, one can obtain the pure relaxation part of acoustic anomalies. However, according to the 3D-Ising model, the resulting values for the relaxation part of attenuation are negative in the temperature range $|T - T_I| < 0.04$ K and thus this possibility was ruled out. For the second case, we have assumed $A^-/A^+ = 1$, which corresponds to mean-field or 3D-XY behavior. The mean-field model gives good results: The relaxational part of the attenuation is shown in Fig. 10 for frequency 31 MHz together with a fit to Eq. (3). The temperature dependence of the attenuation which enters through the relaxation time of the order parameter [Eq. (3)] was taken to be proportional to $(T_I - T)^{-1}$. Since

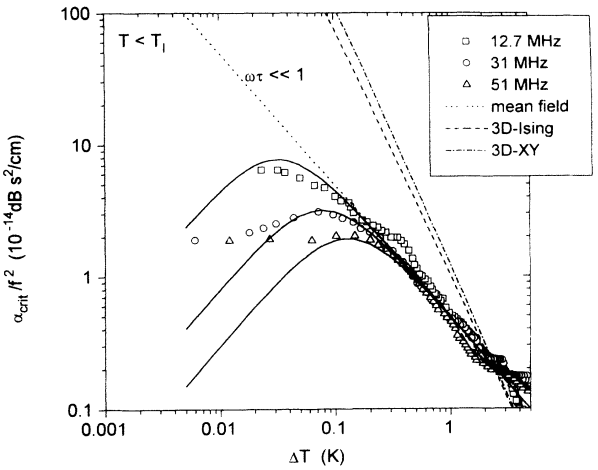

FIG. 9. Critical attenuation vs $\Delta T = T_I - T$ for various frequencies and for $T < T_I$. The dotted line corresponds to $\omega\tau \ll 1$ and has a slope 1. The solid lines are LK fits to the data, with mean-field values for critical exponents. The limit case $\omega\tau \ll 1$ for 3D-Ising and 3D-XY models is also shown.

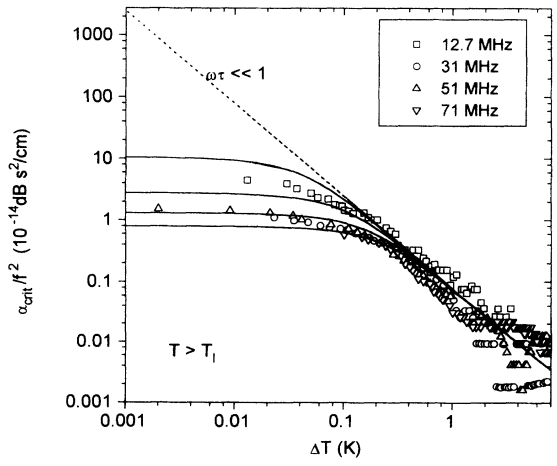

FIG. 8. Critical attenuation vs $\Delta T = T - T_I$ for various frequencies and for $T > T_I$. The fit was carried out with Eq. (8) for data in the $\omega\tau \ll 1$ regime. The solid lines were calculated from Eq. (8) for frequencies 12.7, 31, 51, and 71 MHz using relaxation time $\tau^+ = 6\times 10^{-10}$ s K/$(T-T_I)$.

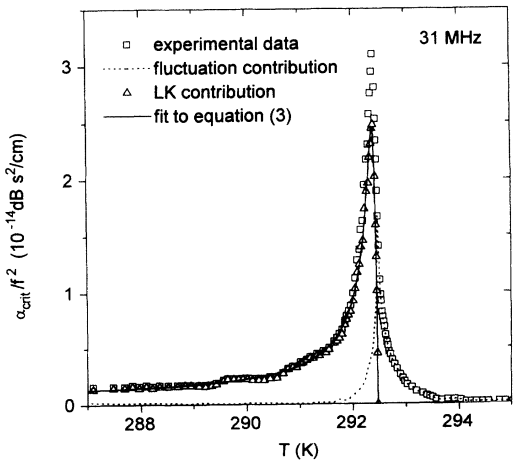

FIG. 10. Pure relaxational part of ultrasonic attenuation (△) in TMATC-Mn for 31 MHz obtained by the subtraction of the fluctuation part (dashed line) from the critical values of attenuation: □, experimental data; solid line, obtained from the fit using Eq. (3).

TABLE I. Fitting parameters used to describe the Landau-Khalatnikov attenuation below $T_I = 292.45$ K. The fit for α/f^2 is based on Eq. (3) with $A = a_1^2 \tau_{A0}/2B\rho v_1^2$.

f (MHz)	Temperature range (K)	A (dB s^2/cm)	τ_{A0} (10^{-10} s K)	Average deviation (dB s^2/cm)
12.7	290.5–292.45	0.393	6.79	0.10
31	284.5–292.45	0.431	4.57	0.02
51	284.5–292.45	0.469	4.35	0.04

most of the data for $T < T_I$ actually belong to the C phase, one should better use $(T_0 - T)^{-1}$. However, because of the smallness of the INC region, the difference in the corresponding exponents is negligible. The corresponding fit parameters of this pure relaxational contribution according to Eq. (3) for measured frequencies 12.7, 31, and 51 MHz are shown in Table I. One can see that the relaxation time of the amplitudon determined by this method is nearly the same as calculated by neglecting the fluctuation effect.

VI. CONCLUSIONS

We have measured the complete set of elastic constants in TMATC-Mn in the temperature range 250–310 K including the normal-incommensurate-commensurate phase transition and the first-order commensurate-commensurate phase transition. We have found that our data can be explained in the frame of the Landau theory including small fluctuations.

At the normal-incommensurate phase transition in TMATC-Mn, we have obtained a frequency dispersion in ultrasonic attenuation near T_I (see Fig. 5). This result shows that the relaxation time of the order parameter (which is the amplitudon in the incommensurate phase) is rather large.

We have determined the relaxation time of the amplitudon as $\tau_A \approx 4 \times 10^{-10}$ s K$/(T_I - T)$. Our result agrees with those in the similar materials TMATC-Zn (Ref. 10) and K_2ZnCl_4 (Ref. 22).

We have tried to describe the critical ultrasonic velocity and attenuation according to the mean-field Landau model, 3D-Ising model, and 3D-XY model. Above T_I, 3D-XY behavior was ruled out and the data could be equally well fitted with 3D-Ising and mean-field theories. Below the lock-in transition T_L, the mean-field theory fits the data best. In the very narrow ($T_I - T_L = 0.6$ K) INC phase, the results are not conclusive.

We have also estimated the relaxation time of the amplitudon, taking into account the fluctuation contribution. The results are similar to the preceding ones, indicating that the fluctuations are not very important for the analysis in the temperature range $T < T_I$.

Concluding, we hope that our results can contribute to a better understanding of the phase transitions not only in TMATC-Mn, but also in other similar materials, and can motivate further experimental and theoretical work in this field.

ACKNOWLEDGMENTS

We acknowledge the experimental help and discussions of Dr. H. Kabelka and general support by Professor H. Warhanek. This work was supported by the Österreichischen Bundesministerium für Wissenschaft und Forschung.

*Permanent address: Department of Physics, Technical University of Transport and Communications, 01026 Zilina, Slovakia.

†Permanent address: Institute of Solid State Physics, Latvian University, 226063 Riga, Latvia.

[1] K. Gesi and K. Ozawa, J. Phys. Soc. Jpn. **53**, 627 (1984).

[2] K. Gesi, Ferroelectrics **66**, 269 (1986).

[3] H. Z. Cummins, Phys. Rep. **185**, 211 (1990).

[4] H. Mashiyama and N. Koshiji, Acta Crystallogr. B **45**, 467 (1989).

[5] H. Mashiyama and S. Tanisaki, J. Phys. Soc. Jpn. **50**, 1413 (1981).

[6] A. Fuith, W. Schranz, H. Warhanek, J. Kroupa, and V. Lhotska, Phase Transit. A **27**, 15 (1990).

[7] O. G. Vlokh, I. I. Polovinko, V. S. Zhmurko, and S. A. Sveleba, Kristallografiya **37**, 525 (1992) [Sov. Phys. Crystallogr. **37**, 273 (1992)].

[8] H. Mashiyama, J. Phys. Soc. Jpn. **49**, 2270 (1980).

[9] O. G. Vlokh, A. V. Kityk, and O. M. Mokryi, Fiz. Tverd. Tela (Leningrad) **32**, 1044 (1990) [Sov. Phys. Solid State **32**, 614 (1990)].

[10] S. M. Silence, K. A. Nelson, and J. Berger, Phys. Rev. B **46**, 2715 (1992).

[11] J. Berger, J. P. Benoit, C. W. Garland, and P. W. Wallace, J. Phys. (Paris) **47**, 483 (1986).

[12] J. O. Fossum, J. Phys. C **18**, 5531 (1985).

[13] P. Kubinec, W. Schranz, and A. Fuith, Acta Phys. Slovaca **43**, 177 (1993).

[14] R. Wyslouzil, Ph.D. thesis, University Vienna, 1985.

[15] E. P. Papadakis, in *Physical Acoustics,* edited by W. P. Mason and R. N. Thurston (Academic, New York, 1976), Vol. 12, p. 279.

[16] A. Sarras and H. Kabelka, Meas. Sci. Technol. (to be published).

[17] R. Truell, Ch. Elbaum, and B. B. Chick, *Ultrasonic Methods in Solid State Physics* (Academic, New York, 1969), Chap. 2.

[18] V. V. Lemanov and S. K. Esayan, Ferroelectrics **73**, 125 (1987).

[19] Y. Ishibashi, in *Incommensurate Phases in Dielectrics,* edited by R. Blinc and A. P. Levanyuk (North-Holland, Amsterdam, 1986), Vol. 2, p. 49.

[20] V. Dvorak and S. K. Esayan, Solid State Commun. **44**, 901 (1982).

[21] J. Hu, J. O. Fossum, C. W. Garland, and P. W. Wallace, Phys. Rev. B **33**, 6331 (1986).

[22] Z. Hu, C. W. Garland, and S. Hirotsu, Phys. Rev. B **42**, 8305 (1990).

[23] A. P. Levanyuk, Zh. Eksp. Teor. Fiz. **49**, 1304 (1965) [Sov. Phys. JETP **22**, 901 (1966)].

[24] R. A. Cowley and A. D. Bruce, J. Phys. C **11**, 3577 (1978).

[25] J. Kroupa, W. Schranz, A. Fuith, H. Warhanek, and P. Saint-Gregoire, Ferroelectrics **125**, 165 (1992).

[26] V. V. Lemanov, Ferroelectrics **78**, 163 (1988).